

ODE-PDE models in traffic flow dynamics

Francesca Marcellini

Abstract. We present two frameworks for the description of traffic flow. First, we consider the coupling of a micro- and a macroscopic models, the former consisting in a system of ordinary differential equations and the latter in the usual LWR conservation law, see [5, 10]. Then, inspired by this model, we consider a macroscopic model where some trajectories are known thanks to, for instance, GPS measurement devices. The result is a new traffic model able to take into account real time data, or, in other words, that encodes these data, see [4]. This work follows a long collaboration with Rinaldo M. Colombo; the author thanks him for his support.

Keywords: macroscopic traffic models, hyperbolic systems of conservation laws.

Mathematical subject classification: 35L65, 90B20.

1 Introduction

We consider mixed systems in the description of dynamics of traffic flow. Differently from the theory of fluid dynamics, traffic dynamics does not rely on well established fundamental principles like the conservation of momentum or energy. Apart from the conservation of the total number of vehicles, the many traffic models available in the literature all have to rely on phenomenological assumptions on the drivers' behavior.

In the current literature, three different approaches are mainly used to model traffic dynamics: microscopic, macroscopic and kinetic. Here, we are concerned with *macroscopic* models, where traffic is described through the fraction $\rho = \rho(t, x)$ of space occupied by vehicles at time t and at position x , and *microscopic* models, consisting of a finite set of ordinary differential equations, describing the motion of each vehicle. For an overview of vehicular traffic models at all scales, we refer to the review papers [1, 2, 3, 6, 11].

The first traffic flow model that we present here is a Micro-Macro model, see [5, 10], consisting of a macroscopic and a microscopic descriptions glued together. The macroscopic part is described through the Lighthill-Whitam [9] and Richards [12] model (LWR),

$$\partial_t \rho + \partial_x (\rho v) = 0 \quad (1.1)$$

given by a scalar conservation law.

The microscopic part is described through a first order Follow-the-Leader (FtL) model, where each driver adjusts his/her velocity to that of the vehicle in front, that is

$$\dot{p}_i = v \left(\frac{\ell}{p_{i+1} - p_i} \right). \quad (1.2)$$

Here, $p_i = p_i(t)$ is the position of the i -th driver, for $i = 1, \dots, n$, and $p_{i+1} - p_i \geq \ell$ for all $i = 1, \dots, n - 1$, the fixed parameter ℓ denoting the (mean) vehicles' length. Here, $\ell/(p_{i+1} - p_i)$ is the local traffic density seen by the driver p_i . Equation (1.2) needs to be closed with the trajectory of the first driver p_n .

We prove the well posedness for this model and we consider a general situation in which the two descriptions (1.1) and (1.2) are alternatively used in different segments of the real line.

The second traffic description that we present here is a new traffic model aware of real time data, see [4].

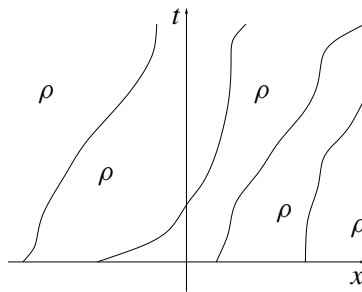


Figure 1: In the macroscopic model (1.3)-(1.4) we assume that some trajectories are known thanks to suitable real time measurements, e.g. GPS devices, while the density $\rho = \rho(t, x)$ is obtained as solution to the PDE (1.3).

Inspired by the above Micro-Macro description, we consider a macroscopic model where some trajectories are known thanks to the present GPS measurement devices that allow a detailed knowledge of the traffic situation essentially in

real time, see Figure 1. This leads to the possibility of improving traffic models by means of real time data.

The model we propose consists of a conservation law of the type

$$\partial_t \rho + \partial_x (\rho \mathcal{V}(t, x, \rho)) = 0 \quad (1.3)$$

where the speed law \mathcal{V} encodes a measured trajectory $p = p(t)$, given by

$$\mathcal{V}(t, x, \rho) = \chi(x - p(t)) \frac{2\dot{p}(t)v(\rho)}{\dot{p}(t) + v(\rho)} + (1 - \chi(x - p(t)))v(\rho). \quad (1.4)$$

We use a time and space dependent speed law that consists of an interpolation between measured data $p = p(t)$ and a *standard* speed law $v = v(\rho)$. It assigns the measured speed $\dot{p}(t)$ near the vehicle providing the data, i.e. for $|x - p(t)| \leq \ell$, and assigns a *standard* speed $v(\rho(t, x))$ far from the measuring vehicle, i.e. when $|x - p(t)| \geq L$. The smooth function $\chi = \chi(\xi)$ attains the value 1 for $|\xi| \leq \ell$ and vanishes when $|\xi| \geq L$, for two fixed constants ℓ, L , with $\ell < L$.

We prove existence, uniqueness and Lipschitz continuous dependence from initial data of the solutions to the Cauchy problem for (1.3)-(1.4) and we note that, from the analytic point of view, the extension to the case of several measured trajectories is of a merely technical nature.

In the next section we present the Micro–Macro description; in Section 3 we present the traffic model aware of real time data and the last section is devoted to a few numerical integrations, which show qualitative properties of the solutions of the two different traffic descriptions.

2 Micro-Macro Description

From a macroscopic point of view, vehicular traffic can be viewed as a compressible fluid flow, whereas a microscopic approach describes the behavior of each individual vehicle. None of the two approaches is separately able to capture the information of traffic dynamics. In fact, macroscopic models allow to simulate traffic on large networks but do not take much account of the details. On the other hand, microscopic models can cover such details, but they are not tractable on a large network. A natural strategy is therefore to combine macroscopic and microscopic models.

Below, we give some notations and a well posedness result for the LWR-FtL case, when the LWR model describes the traffic dynamics on the right and the FtL on the left. Our aim is to consider a general situation, in which the two descriptions (1.1) and (1.2) are alternatively used in different segments of the

real line. This is because the point of cohesion of the two frameworks is not fixed. The case FtL-LWR, when the FtL model describes the traffic dynamics on the right and the LWR on the left, and the general case are presented in [5, Sections 2.2 and 2.3].

Throughout, we denote $\mathbb{R}^+ = [0, +\infty[$ and $\mathring{\mathbb{R}}^+ =]0, +\infty[$. For any $n \in \mathbb{N}$ and $\ell \in \mathring{\mathbb{R}}^+$, the set of admissible positions of n vehicles of length ℓ is

$$\mathcal{P}_\ell^n = \left\{ p \in \mathbb{R}^n : p_{i+1} - p_i \geq \ell \text{ for } i = 1, \dots, n - 1 \right\}. \tag{2.1}$$

We assume the following condition on the speed law:

(v) $v \in \mathbf{C}^2([0, 1]; \mathbb{R}^+)$ is strictly decreasing, with $v(1) = 0$ and is such that $\frac{d^2}{d\rho^2}(\rho v(\rho)) < 0$.

Let n vehicles start at time $t = 0$ from positions $\bar{p} \in \mathcal{P}_\ell^n$ and use the LWR model to describe the traffic dynamics for $x < \bar{p}_1$. The system is the following:

$$\left\{ \begin{array}{ll} \partial_t \rho + \partial_x(\rho v(\rho)) = 0 & t \in \mathbb{R}^+ \text{ and } x < p_1(t) \\ \dot{p}_i = v\left(\frac{\ell}{p_{i+1} - p_i}\right) & t \in \mathbb{R}^+ \text{ and } i = 1, \dots, n - 1 \\ \dot{p}_n = w(t) & t \in \mathbb{R}^+ \\ \rho(0, x) = \bar{\rho}(x) & x \leq \bar{p}_1 \\ p(0) = \bar{p} \end{array} \right. \tag{2.2}$$

where $w \in \mathbf{L}^\infty(\mathbb{R}^+; \mathbb{R}^+)$ is the speed of the first driver, that is the leader, $\bar{\rho} \in (\mathbf{L}^1 \cap \mathbf{BV})(\mathbb{R}; [0, 1])$ describes the vehicles' distribution for $x < \bar{p}_1$ and $\bar{p} \in \mathcal{P}_\ell^n$. In system (2.2), the trajectory of p_1 acts as a boundary between the microscopic model on its right and the macroscopic one on its left.

A solution to (2.2) on the time interval $[0, T[$, consists of map

$$\rho \in \mathbf{C}^0([0, T]; (\mathbf{L}^1 \cap \mathbf{BV})(\mathbb{R}; [0, 1])) \text{ with } \rho(t, x) = 0 \text{ whenever } x < p_1(t)$$

$$p \in \mathbf{W}^{1,\infty}([0, T]; \mathbb{R}^n).$$

The following result holds:

Proposition 2.1. *Fix $\ell > 0$, $V > 0$, $n \in \mathbb{N}$ with $n \geq 2$ and a v that satisfies (v). Let w be in $\mathbf{L}^\infty(\mathbb{R}^+; [0, V])$. For any $\bar{p} \in \mathcal{P}_\ell^n$ and for any $\bar{\rho} \in (\mathbf{L}^1 \cap \mathbf{BV})(\mathbb{R}; [0, 1])$, problem (2.2) admits a unique solution. Moreover, there exists a positive L such that if $w' \in \mathbf{L}^\infty(\mathbb{R}^+; [0, V])$, $\bar{p}' \in \mathcal{P}_\ell^n$ and $\bar{\rho}' \in$*

$(\mathbf{L}^1 \cap \mathbf{BV})(\mathbb{R}; [0, 1])$, then the corresponding solutions (p, ρ) and (p', ρ') satisfy for all $t \geq 0$ the following estimates:

$$\begin{aligned} \|\rho(t, \cdot) - \rho'(t, \cdot)\|_{\mathbf{L}^1} &\leq L \|\bar{\rho} - \bar{\rho}'\|_{\mathbf{L}^1} + L \left(1 + (1 + 2V) \frac{2}{\ell} t\right) \\ &\quad \times \left(\|\bar{p} - \bar{p}'\| + \|w - w'\|_{\mathbf{L}^1((0,t])}\right) \exp \left[2 \frac{\mathbf{Lip}(v)}{\ell} t\right] \\ \|p(t) - p'(t)\| &\leq \left(\|\bar{p} - \bar{p}'\| + \|w - w'\|_{\mathbf{L}^1((0,t])}\right) \exp \left(2 \frac{\mathbf{Lip}(v)}{\ell} t\right). \end{aligned}$$

For the proof see [5, Proposition 2.2].

3 A Traffic Model Aware of Real Time Data

In this section we present a traffic model aware of real time data, or, in other words, that encodes real data coming from GPS measurement devices.

From an analytic point of view, a justification of our insertion of real time traffic data in the formulation of the model is provided by the difficulties inherent to the solution of the inverse problem for a 1D scalar conservation law. Indeed, a rigorous approach to the issue of finding the “right” speed law $\mathcal{V} = v(\rho)$ leads to an inverse problem that can be stated as follows. Find the function $\mathcal{V} = v(\rho)$ so that the solution to (1.3) best approximates the observed traffic dynamics. More formally, we are led to consider the following inverse problem:

$$\begin{aligned} \text{find } v \text{ so that } \int_0^T |\dot{p}(t) - v(\rho(t, p(t)+))| dt \text{ is minimal,} \\ \text{where } \begin{cases} \partial_t \rho + \partial_x (\rho v(\rho)) = 0 \\ \rho(0, x) = \rho_0(x) \end{cases} \end{aligned} \tag{3.1}$$

At first, we show that problem (4.1) is in general ill posed. Indeed, we consider the Riemann Problem

$$\begin{cases} \partial_t \rho + \partial_x (\rho v_\varepsilon(\rho)) = 0 \\ \rho(0, x) = \begin{cases} 1/8 & x < 0 \\ 3/8 & x > 0 \end{cases} \end{cases} \tag{3.2}$$

and, for $\varepsilon \in [-1, 1]$, we consider the following speed law and the corresponding flow

$$v_\varepsilon(\rho) = (1 + \varepsilon\rho)(1 - \rho) \quad \text{and} \quad f_\varepsilon(\rho) = (1 + \varepsilon\rho)(1 - \rho)\rho \tag{3.3}$$

and choose the trajectory $p(t) = t/2$.

The discrepancy between measured data and the description provided by the LWR model can be estimated through straightforward computations as follows:

$$\int_0^T |\dot{p}(t) - v_\varepsilon(\rho_\varepsilon(t, p(t)))| dt = \begin{cases} \left(\frac{9}{8} + \frac{15\varepsilon}{64}\right) T & \text{if } \varepsilon \leq 0 \\ \left(\frac{3}{8} + \frac{7\varepsilon}{64}\right) T & \text{if } \varepsilon > 0 \end{cases}$$

This shows that the map

$$\begin{aligned} \varphi: [-1/3, 1/3] &\rightarrow \mathbb{R} \\ \varepsilon &\rightarrow \int_0^T |\dot{p}(t) - v_\varepsilon(\rho_\varepsilon(t, p(t)))| dt \end{aligned} \tag{3.4}$$

does not attain a minimum, see Figure 2.

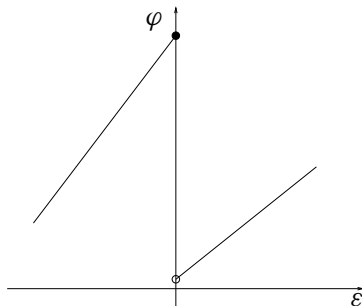


Figure 2: The map φ defined in (3.4) does not attain a minimum for $\varepsilon \in [-1/3, 1/3]$. Above, $\varphi(0+) = 3/8$ and $\varphi(0-) = 9/8$.

Moreover, a positive result in this direction is also obtained in [4, Proposition 2.2]. We consider problem (4.1) in a specific class of speed laws, that is

$$v_V(\rho) = V(1 - \rho) \tag{3.5}$$

with $V \in [\check{V}, \hat{V}]$ being the maximal speed of cars along the considered road.

We consider a measured trajectory $p \in \mathbf{W}^{1,\infty}$ and the following Cauchy problem

$$\begin{cases} \partial_t \rho_V + \partial_x \left(\rho_V V (1 - \rho_V) \right) = 0 \\ \rho_V(0, x) = \rho_o(x) \end{cases} \tag{3.6}$$

where $\rho_o \in (\mathbf{L}^1 \cap \mathbf{BV})(\mathbb{R}; [0, 1])$. In [4, Proposition 2.2] we prove that the map

$$\begin{aligned} \mathcal{E}: [\check{V}, \hat{V}] &\rightarrow \mathbb{R} \\ V &\rightarrow \int_0^T \left| \dot{p}(t) - v_V \left(\rho_V(t, p(t)) \right) \right| dt \end{aligned}$$

is continuous, provided the following two assumptions

$$\text{essinf}_{x \in \mathbb{R}} \rho_o > \check{\rho} \quad \text{and} \quad \text{essinf}_{t \in [0, T]} \dot{p} \geq \hat{V}(1 - 2\check{\rho}). \tag{3.7}$$

The above result relies on assumptions that can be hardly acceptable in a real situation. Thus we propose the new model aware of real time data in (1.3)-(1.4) and, more precisely, we consider the following Cauchy Problem

$$\begin{cases} \partial_t \rho + \partial_x (\rho \mathcal{V}(t, x, \rho)) = 0 \\ \rho(0, x) = \rho_o(x) \end{cases} \tag{3.8}$$

where $\rho_o \in \mathbf{L}^\infty(\mathbb{R}; [0, 1])$ and

$$\mathcal{V}(t, x, \rho) = \chi(x - p(t)) \frac{2\dot{p}(t)v(\rho)}{\dot{p}(t) + v(\rho)} + (1 - \chi(x - p(t)))v(\rho). \tag{3.9}$$

We posit below the following assumptions on the functions appearing in (3.8)-(3.9).

(v) $v \in \mathbf{C}^{0,1}([0, 1]; [0, V])$ is such that

$$\left\{ \begin{array}{ll} v(1) = 0 & \\ \rho \rightarrow v(\rho) & \text{is non increasing,} \\ \rho \rightarrow \rho v(\rho) & \text{is strictly concave,} \\ \rho \rightarrow \frac{\rho w v(\rho)}{w + v(\rho)} & \text{is strictly concave, } \forall w > 0. \end{array} \right.$$

(p) $p \in \mathbf{C}^{1,1}(\mathbb{R}^+; \mathbb{R})$ is such that $\dot{p} \geq 0$ for a.e. $t \in \mathbb{R}^+$.

(χ) $\chi \in \mathbf{C}_c^1(\mathbb{R}^+; [0, 1])$.

The main result is given by

Theorem 3.1. *Let (v), (p) and (χ) hold. Then, for any $\rho_o \in \mathbf{L}^\infty(\mathbb{R}; [0, 1])$, problem (3.8)–(3.9) admits a unique Kružkov solution. Moreover, if $\rho'_o \in \mathbf{L}^\infty(\mathbb{R}; [0, 1])$ is another initial datum and $\rho = \rho(t, x)$, $\rho' = \rho'(t, x)$ are the*

solutions corresponding to the initial data $\rho_o \rho'_o$, the following Lipschitz estimate holds:

$$\|\rho'(t) - \rho(t)\|_{L^1(\mathbb{R};\mathbb{R})} \leq e^{Ct} \|\rho'_o - \rho_o\|_{L^1(\mathbb{R};\mathbb{R})}, \tag{3.10}$$

where

$$C = \mathbf{Lip}(\chi) (1 + \mathbf{Lip}(p)) (\mathbf{Lip}(p)L + \mathbf{Lip}(\rho v)) + \mathbf{Lip}(g)\mathbf{Lip}(\dot{p}) \tag{3.11}$$

is independent from ρ_o and ρ'_o .

For the definition of Kruřkov solution see [4, Definition 3.1] or [7, Definition 1]. For the proof see [4, Section 5].

4 Numerical Integrations

To numerically integrate the Micro-Macro model in (2.2) we use the Lax-Friedrichs algorithm, see [8, Section 12.1], for the partial differential equation and the explicit forward Euler method for the ordinary differential equation.

We choose

$$v(\rho) = 1 - \rho, \quad \ell = 0.49 \quad \text{and} \quad w(t) = 0.75 \tag{4.1}$$

with initial datum

$$\bar{\rho}(x) = 0.8 \chi_{[-9,-7]}(x) + 0.6 \chi_{[-7,-6]}(x) + \chi_{[-4,-0.5]}(x) \tag{4.2}$$

$$\bar{p} = [0, 0.5, 1., 1.5, 2., , 2.5, 3., 3.5, 4., 4.5, 5., 7., 8., 9., 10.]$$

The resulting solution is displayed in the (t, x) plane in Figure 3. It was computed with a space mesh size $\Delta x = 2.5 \times 10^{-3}$ and a time mesh size updated at each time step $\Delta t = 0.9 \cdot \Delta x / \Lambda$, where Λ is the maximal characteristic speed.

In Figure 3, on the left, we see the typical behavior of the solutions to the LWR model, consisting of shocks and rarefaction waves. On the right, the microscopic part yields the trajectories of the single vehicles. The leftmost drivers in the microscopic phase have a very low initial speed. Hence, the rightmost vehicles in the macroscopic phase have to brake at about $t = 0.5$, forming a queue. Later, the drivers in the microscopic phase accelerate and this increase in the speeds reaches also the macroscopic phase.

To numerically integrate the model aware of real time data in (3.8)-(3.9) we use the standard Lax-Friedrichs algorithm, see [8, Section 12.1]. Also in this case we use a fixed space mesh size $\Delta x = 2.5 \times 10^{-3}$.

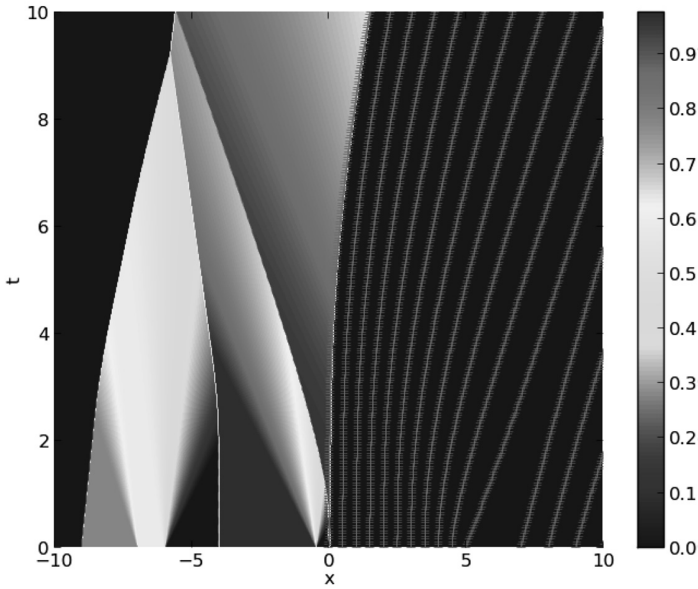


Figure 3: Numerical integration of the LWR-FtL model (2.2)-(4.1)-(4.2).

As a first example, in Figure 4, we choose the speed law

$$v(\rho) = 1 - \rho \tag{4.3}$$

and the constant initial datum

$$\rho_o(x) = 0.5 . \tag{4.4}$$

We consider a car p , which we imagine equipped with a GPS measuring device, that follows the trajectory

$$\begin{aligned} \dot{p}(t) = & 0.5 \chi_{[0,5]}(t) + 0.6 \chi_{[5,6]}(t) + 0.2 \chi_{[8,11]}(t) \\ & + 0.4 \chi_{[13,18]}(t) , \quad p(0) = 0 . \end{aligned} \tag{4.5}$$

In the time interval $[0, 5]$, the speed of p equals that resulting from the LWR model at the initial density (4.4). Therefore, the measuring car has no effects on the evolution prescribed by the partial differential equation, see Figure 4. The model allows to observe queues unpredictable for the LWR model, thanks to the real time data provided by p . Behind the measuring car, the maximal density is reached, while in front of this the road empties.

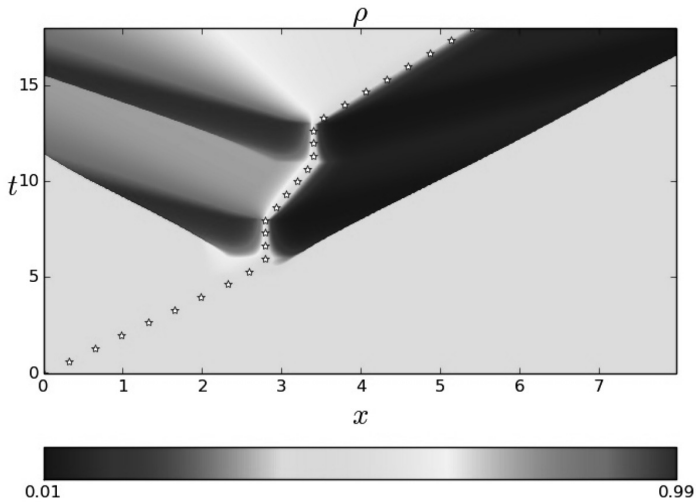


Figure 4: Numerical integration of the model (3.8)-(3.9)-(4.4)-(4.5). For $t \in [0, 5]$, the knowledge of the trajectory of p has no effects on the LWR description. For $t > 5$, the effects of the jams revealed by the car is evident.

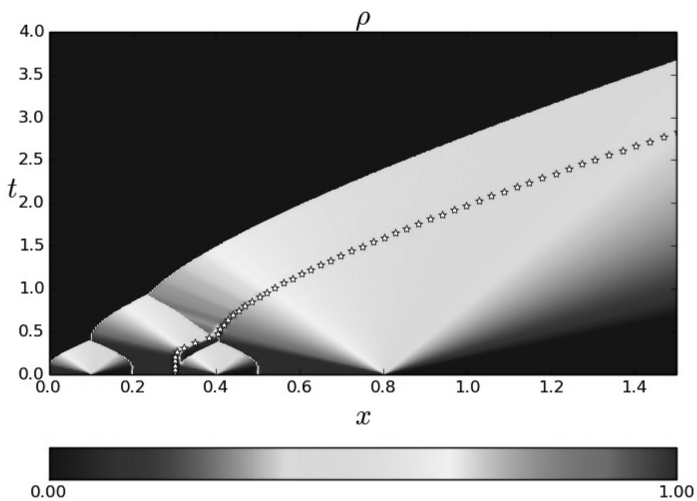


Figure 5: Numerical integration of (3.8)-(3.9)-(4.6) with $\dot{p} = v(\rho(t, p(t+)))$, resulting in the usual LWR evolution.

Then, in Figure 5, we choose the non constant initial datum

$$\rho_o(x) = \chi_{[0.001,0.1]}(x) + \chi_{[0.2,0.4]}(x) + \chi_{[0.5,0.8]}(x) \tag{4.6}$$

for (1.3) and assign to the unique measuring vehicle p the speed resulting from the speed law (4.3). The evolution prescribed by (1.4) is the same as the one provided by the LWR model.

Assume now that at time $t = 1.0$ the measuring car slows down to speed 0.2, causing a queue behind and a free region in front. Then, for $t \in [1.5, 2.5]$ it stops, so that the density behind it reaches the maximum possible value. This behavior might be caused, for instance, by some sort of accident. Then, at $t = 2.5$, the measuring car restarts traveling with the LWR speed, see Figure 6.

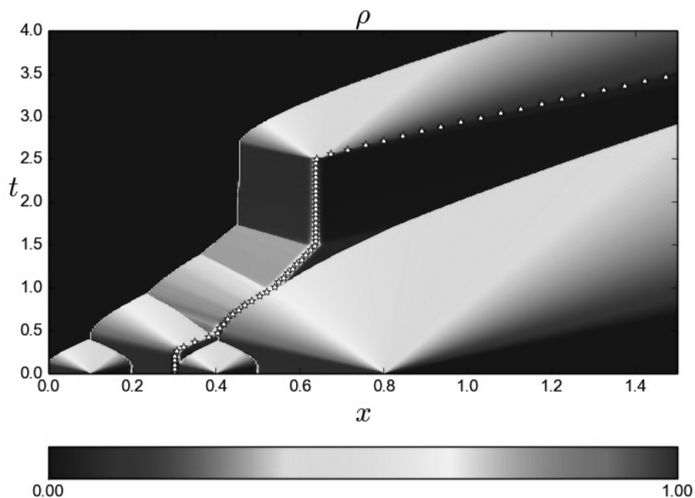


Figure 6: Here, the measured data are very different from the predictions of the LWR model. The measuring vehicle p moves according to $\dot{p} = v(\rho(t, p(t)+))$ for $t \in [0, 1.0]$, slows down to speed 0.2 for $t \in [1.0, 1.5]$, stops at $t = 1.5$ due to, say, an accident, and finally resumes the LWR speed for $t > 2.5$. The model (3.8)-(3.9)-(4.6) is able to describe the resulting queues.

This example shows that, in spite of the impossibility of a deterministic forecast of the insurgence of road accidents, the present model is able to take into account the consequences of such an event, taking advantage of the present day technologies and realistically describing the corresponding effects.

Acknowledgment. This research follows a long collaboration with Rinaldo M. Colombo; the author thanks him for his support. Moreover the author acknowledges the support given by the HYP2014 organization, that enabled her participation to the meeting, and that one given by the INdAM–GNAMPA 2014 project *Conservation laws in the modeling of collective phenomena*.

References

- [1] N. Bellomo, A. Bellouquid, J. Nieto and J. Soler. *On the multiscale modeling of vehicular traffic: From kinetic to hydrodynamics*. Discrete Contin. Dyn. Syst. Ser. B, **19**(7) (2014), 1869–1888.
- [2] N. Bellomo and C. Dogbe. *On the modeling of traffic and crowds: a survey of models, speculations, and perspectives*. SIAM Rev., **53**(3) (2011), 409–463.
- [3] A. Bressan, S. Čanić, M. Garavello, M. Herty and B. Piccoli. *Flows on networks: recent results and perspectives*. EMS Surv. Math. Sci., **1**(1) (2014), 47–111.
- [4] R.M. Colombo and F. Marcellini. *A traffic model aware of real time data*. Mathematical Models and Methods in Applied Sciences, (2015), DOI: 10.1142/S0218202516500081, to appear.
- [5] R.M. Colombo and F. Marcellini. *A mixed ODE-PDE model for vehicular traffic*. Mathematical Methods in the Applied Sciences, **38** (2015), 1292–1302.
- [6] A. Klar and R. Wegener. *Traffic flow: models and numerics*. In “Modeling and computational methods for kinetic equations”, Model. Simul. Sci. Eng. Technol., pages 219–258. Birkhäuser (2004).
- [7] S.N. Kružhkov. *First order quasilinear equations with several independent variables*. Mat. Sb. (N.S.), **81**(123) (1970), 228–255.
- [8] R.J. LeVeque. *Numerical methods for conservation laws*. Lectures in Mathematics ETH Zürich. Birkhäuser Verlag, Basel, second edition (1992).
- [9] M.J. Lighthill and G.B. Whitham. *On kinematic waves. II. A theory of traffic flow on long crowded roads*. Proc. Roy. Soc. London. Ser. A., **229** (1955), 317–345.
- [10] F. Marcellini. *Free-congested and micro-macro descriptions of traffic flow*. Discrete Contin. Dyn. Syst. Ser. S, **7**(3) (2014), 543–556.
- [11] B. Piccoli and A. Tosin. *Vehicular traffic: a review of continuum mathematical models*. Encyclopedia of Complexity and Systems Science. Springer, New York, **22** (2009), 9727–9749.
- [12] P.I. Richards. *Shock waves on the highway*. Operations Res., **4** (1956), 42–51.

Francesca Marcellini

Dip. di Matematica e Applicazioni
Università di Milano – Bicocca
Via Cozzi, 55
20125 Milano
ITALY

E-mail: francesca.marcellini@unimib.it